Native fluorescence spectra of human cancerous and normal breast tissues analyzed with non-negative constraint methods

Yang Pu, Wubao Wang, Yuanlong Yang, and Robert R. Alfano*

Institute for Ultrafast Spectroscopy and Lasers, Department of Physics, City College of the City University of New York, 160 Convent Avenue, New York 10031, USA

*Corresponding author: ralfano@sci.ccny.cuny.edu

Received 22 October 2012; revised 28 November 2012; accepted 21 December 2012; posted 18 January 2013 (Doc. ID 178439); published 18 February 2013

The native fluorescence spectra of human cancerous and normal breast tissues were investigated using the selected excitation wavelength of 340 nm to excite key building block molecules, such as reduced nicotinamide adenine dinucleotide (NADH), collagen, and flavin. The measured emission spectra were analyzed using a non-negative constraint method, namely multivariate curve resolution with alternating least-squares (MCR-ALS). The results indicate that the biochemical changes of tissue can be exposed by native fluorescence spectra analysis. The MCR-ALS-extracted components corresponding to the key fluorophores in breast tissue, such as collagen, NADH, and flavin, show differences of relative contents of fluorophores in cancerous and normal breast tissues. This research demonstrates that the native fluorescence spectroscopy measurements are effective for detecting changes of fluorophores composition in tissues due to the development of cancer. Native fluorescence spectroscopy analyzed by MCR-ALS may have the potential to be a new armamentarium.

OCIS codes: 170.0170, 170.6510, 300.0300, 300.6170.

1. Introduction

Breast cancer is the second most common malignant tumor among women throughout the world [1]. It was estimated that 226,870 new cases of invasive breast cancer occurred among women and about 39,920 women died of breast cancer in the U.S. in 2012 [1]. Breast cancer can be classified by different schemata, including stage, pathology, grade, receptor status, and the presence or absence of specific genes determined by DNA tests [2–7]. In 1984, "optical biopsy" was introduced by a group at the City College of New York (CCNY) to investigate tissue using ultraviolet (UV) to visible light, which has the potential to diagnose diseases without removing tissue samples [8]. Since the pioneering reports on the laser-induced fluorescence of biological tissues in the mid-1980s [8,9], optical spectroscopy has been widely used for diagnostic purposes for cancer [10–13] and other diseases. Although there is a lot of experimental evidence indicating differences of fluorescence spectra between cancerous and normal tissues [8,9], few works disclose the biological basis of these differences and study the key building block molecules contributing to the fluorescence of tissue.

In the evaluation of fluorescence diagnosis, there are two major problems hampering the reliability of extracting the differences of the biochemical and/or morphological properties between cancerous and normal samples. One is that the differences existing among each type of tissue samples from different patients make it difficult to control the same measuremental condition for each type (cancerous or normal) of tissue samples. Another problem is the presence of significant spectral distortions induced by endogenous absorber and scatterer [11]. The first causes unreliability in directly comparing the emission intensities of

1559-128X/13/061293-09$15.00/0

one certain biomarker [such as nicotinamide adenine dinucleotide (NADH)] between individual cancerous and normal breast samples [11]. The second induces imperfection in reconstructing the emission spectra of tissue using the known measured spectra of key individual fluorophores [11].

To evaluate the relative contents of bimolecular components in tissue, a blind source separation (BSS) method, namely multivariate curve resolution with alternating least-squares (MCR-ALS), may be used to extract the intrinsic (undistorted) fluorescence spectrum of each principal biochemical (fluorophore) from the mixed spectra. The principle of the MCR-ALS method was described in detail by Tauler *et al.* [14]. It was developed for the recovery of the response profiles (spectra, pH profiles, time-resolved profiles, etc.) of more than one components in an unresolved and/or unknown mixture when little or no information is known about these mixtures. In spectral analysis, the MCR-ALS method is superior to other BSS methods, such as principal component analysis, independent component analysis, and factor analysis because (1) spectral data and the contents of constituents generated from the MCR-ALS analysis give positive values; therefore, it is better to use the non-negativity constraint analysis since this tool may extract the true spectrum of each biochemical in tissue from the measured entire tissue emission data [14] and (2) hidden constituents in the mixed compound such as tissue may show different spectra other than pure biochemicals because of the complex surroundings, but the spectra decomposed by the MCR-ALS analysis may find the "real" spectra in mixed environment.

The focus of the present research is to study whether the native fluorescence spectroscopy measurements analyzed with the MCR-ALS method are effective to detect changes of the native fluorophores' contents related to variation of normal breast tissue to malignant tissue. The excitation at 340 nm is the prime focus here due to (1) its lower toxicity effect for inducing cancer than using excitation wavelengths shorter than 300 nm [15] and (2) the effective excitation of the three building block molecules in tissue, such as collagen, NADH, and flavin. The basic fluorescence spectrum and relative content of each key fluorophore in human breast tissue were calculated using the measured tissue spectra and the MCR-ALS method by treating spectra of different fluorophores as the PCs contributing to the tissue spectra. The linear discriminant analysis (LDA) was then used to analyze biomolecular alterations reflected in the native fluorescence spectra of cancerous and normal breast tissues and obtain criteria for separating these two types of tissues using fluorescence spectra data. Subsequently, the receiver operating characteristic (ROC) curves were generated to evaluate the performance of the MCR-ALS algorithm combined with LDA for diagnosis of human breast cancer. Our experimental and analysis results demonstrate how the native fluorescence spectroscopy can be used to detect the changes of fluorophore contents due to cancer formation. The native fluorescence spectroscopic technique may be used to diagnose disease without removing tissue samples, heading toward new advanced tools for medical armamentarium.

2. Material and Method

Pairs of cancerous and normal breast tissue samples were provided by the Co-operation Human Tissue Network (CHTN) and the National Disease Research Interchange (NDRI) under the approval of the CCNY Institutional Review Board. The cancerous and normal breast tissue samples were diagnosed by pathology medical doctors. Samples were neither chemically treated nor frozen prior to the experiments. The time elapsed between tissue resection and the fluorescence measurements may vary for different sample sources. The longest elapsed time is about 30 hours. Fluorescence measurements were performed on breast tissue samples using a Perkin-Elmer LS-50 spectrometer. In the spectrometer, an equipped Xenon lamp coupled with narrow band filter was used as light source to illuminate the sample at a desired wavelength, and the fluorescence emitted from the sample is collected by an emission monochromator connected to a photomultiplier tube. The excitation light with 5 nm spectral width was focused on samples with spatial size of $\sim 3 \times 1$ mm. The power of incident light was ~ 0.5 μW. The scan speed was 250 nm per minute. The fluorescence was collected with a resolution of ~ 0.5 nm from the front face of tissue samples to reduce the distortion of absorption and scattering, which is often done for turbid or opaque samples [12]. The fluorescence spectra of 38 pairs of cancerous and normal breast tissues were recorded and analyzed. The breast tissue samples used for fluorescence measurements were cut into $\sim 1.5 \times \sim 1 \times \sim 0.3$ cm (length × width × thickness) pieces. To eliminate the possible spectral differences among different areas of each individual tissue sample, the emission of two or three spots from one breast tissue was measured and their averages taken as the measured fluorescence contributed from that sample. In order to study changes of relative contents of collagen and NADH due to cancer formation, the fluorescence spectra of cancerous and normal breast tissues were measured with selected excitation wavelength of 340 nm, which is close to the absorption peaks of these fluorophores. The fluorescence of other fluorophores in tissue obtained with the selected excitation wavelength of 340 nm is expected to have much lower intensity since their absorption peaks are far away from 340 nm.

In this study, the MCR-ALS analysis was used to extract the undistorted fluorescence spectrum of each principal biochemical component [13,14] from the spectra of the breast tissue samples and the relative contents of the principal biochemical components. The MCR-ALS analysis is briefly described as $\mathbf{D} = \mathbf{C}\mathbf{S}^{\mathbf{T}} + \mathbf{E}$, where D is the data matrix containing

experimental spectra in rows; C is the matrix of calculated content profiles; S^T is the matrix of calculated spectra of components contributed to D; and E is the residual error matrix between D and CS^T [13,14]. In order to obtain a physical and/or biological meaning, the MCR-ALS analysis was achieved to approach diverse constraints (non-negativity, unimodality, selectivity, closure, etc.) using a group of methods (such as least squares calculation, PC analysis, or evolving factor analysis method) during the iterations [14].

LDA is one of the most well-known and powerful classifiers. By using a group fluorescence spectra of cancerous and normal tissues as training data [16], a classifier expressed by a linear separating line $y = ax + b$ in the subspace of relative contents of paired fluorophores was obtained. These separating lines were evaluated as diagnostic criteria by a set of testing data other than the training data. To optimize a better criterion of the separating line, the LDA was employed to all data, including the training and testing (evaluated) data, to generate an updated separating line. ROC testing was also conducted to further evaluate the performance of the LDA algorithms on native fluorescence spectra for breast cancer detection.

3. Experimental Results

The emission spectra of the key fluorophores of interest, collagen, NADH, flavin, tryptophan, and elastin, were measured individually with the excitation at 340 nm, and the results were reported in our previous work [12]. Each soluble fluorophore was prepared in aqueous solution in quartz cell with the same concentration of ~0.5 mg/ml. An insoluble fluorophore, such as collagen, was prepared as an aqueous suspension and shaken evenly before the measurements. The absorption and emission peaks of the key fluorophores of interest are concluded in Table 1.

Under 340 nm excitation, the emission of collagen, elastin, NADH, and flavin can be measurable while the emission intensities from other fluorophores are much weaker than these four principal fluorophores. The component with strongest fluorescence other than the principal four is tryptophan. However, its intensity is just less than 2% of the intensity from collagen. This can be understood because the absorption peak of tryptophan is located at ~280 nm, far from the excitation wavelength of 340 nm [12]. The strong emission of collagen and NADH comes from the resonant excitation at 340 nm. Since the absorption peaks of elastin and flavin are located at 351 and 375 nm, respectively, which are at the lower energy side of the 340 nm photon, they should also have enough emission under excitation of 340 nm. Therefore, it can be expected that the spectra obtained with excitation of 340 nm for breast tissues, as shown in Fig. 1, were mainly contributed from collagen, elastin, NADH, and flavin.

Table 1. Absorption and Emission Peaks of the Key Fluorophores of Interest

	Fluorophores				
Spectral Type	Tryptophan	Collagen	Elastin	NADH	Flavin
Absorption (nm)	280	339	351	340	375
Emission (nm)	342	380	410	460	525

Differences of the emission spectra between the cancerous and normal tissue samples were reproducibly observed in the spectral range from ~360 nm to ~580 nm. The average fluorescence spectral profiles of the cancerous (solid line) and normal (dashed line) breast tissues obtained with the selected excitation at 340 nm are shown in Fig. 1. The standard deviation error bars are also indicated in Fig. 1. Each spectral profile was normalized to unit value of 1 (i.e., the sum of squares of the data elements in each emission spectrum was set as 1) before taking averaging. The main emission peaks of both cancerous and normal breast tissues are found approximately at 380 nm. The major difference of the fluorescence spectral profiles of the cancerous and normal tissues is the existence of a higher shoulder peak at ~460 nm for the cancerous tissue while emission intensity of normal tissue decays somehow monotonously with the wavelength after the main peak. This difference indicates the change of fluorophore compositions in tissue during the tumor development. In addition, a tiny local plateau at 539 nm may be observed in the emission spectra of both cancerous and normal breast tissues, which is known as the characteristic peak of flavin.

The native fluorescence spectra of cancerous and normal breast tissues were analyzed using the MCR-ALS method to (1) understand and extract the changes of relative contents of principal biochemical components in the cancerous and normal breast tissues and (2) create a criterion that can be used to distinguish cancerous breast tissue from normal tissue.

The spectra of 22 cancerous and normal breast tissues were randomly chosen from the total 38 samples to be analyzed using the MCR-ALS method to extract the spectrum of each PC and its contribution to the tissue fluorescence spectra and generate a criterion for breast cancer detection.

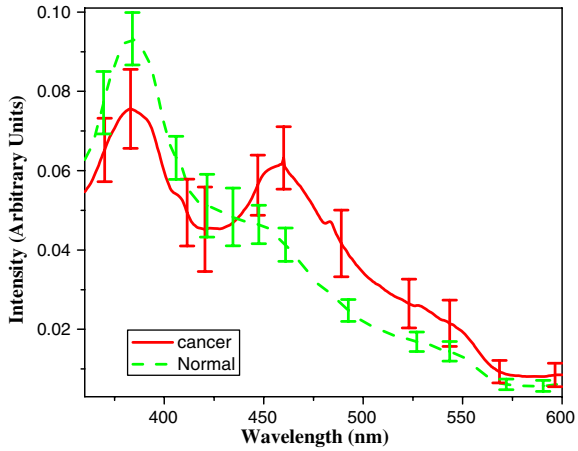

Fig. 1. (Color online) Average fluorescence spectra of cancerous (solid) and normal (dash) breast tissues obtained with the selective excitation wavelength of 340 nm.

The MCR-ALS analysis could not distinguish between collagen and elastin and takes them as the same component since their emission peaks are very close at ~390–400 nm and these two biomolecules have similar emission spectral profile. The decomposed spectra of principal fluorophores and the corresponding measured fluorophores' spectra are shown in Fig. 2, as solid and dashed lines, respectively, where the first component stands for collagen, the second for NADH, and the third for flavin. The PCs correspond to fluorescence peaks as follows: the peak at ~385 nm is contributed from collagen and/or elastin, the peak at ~461 nm is contributed from NADH, and the peak at ~523 nm is contributed from flavin. It can be seen that the retrieved spectrum for each decomposed component is in good agreement with the corresponding measured fluorophore's spectrum, which demonstrates that the MCR-ALS method accounts for the major spectroscopic feature of the mixed fluorophores [14]. The differentiation between the extracted individual fluorophore's fluorescence spectrum and the measured spectrum of the corresponding individual fluorophore was observed, which can be explained mainly from distortions caused by tissue scattering and absorption [10].

To characterize changes of the relative contents of the PCs (fluorophores), the relative contents of collagen and/or elastin, NADH, and flavin in the cancerous and normal breast tissues were extracted using the MCR-ALS method by treating collagen (elastin), NADH, and flavin as three PCs. Figure 3(a) shows the relative content of the first component (collagen) versus the second component (NADH), and Fig. 3(b) displays the relative content of the second component (NADH) versus the third component (flavin) of cancerous (circle) and normal (square) breast tissues. The most salient feature of Fig. 3(a) is that all data points for the cancerous tissues are located in the left-upper side of the data points for the normal tissues, indicating that the relative content of NADH is higher in cancerous tissues in comparison with the normal tissues while the relative content of collagen

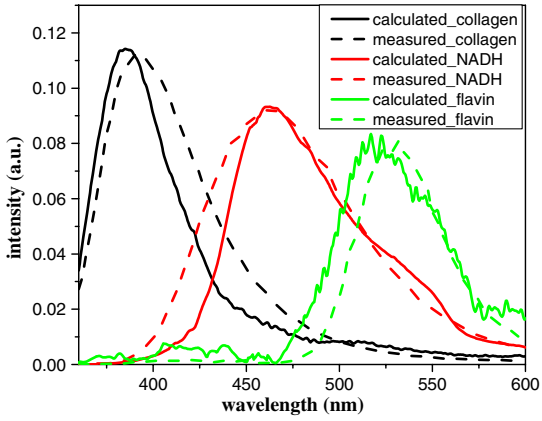

Fig. 2. (Color online) Comparison of spectra of three PCs (solid) extracted from the fluorescence spectra of breast tissue using the MCR-ALS method and the measured (dash) spectra of individual collagen (elastin), NADH, and flavin.

is lower in cancerous tissues than the normal tissues. Figure 3(b) shows that all data points for the cancerous tissues are located in the right-upper side of data points for the normal tissues, indicating that the relative content of NADH and flavin is higher in cancerous tissues in comparison with the normal tissues. It can be seen from Figs. 3(a) and 3(b) that the relative content of collagen in cancerous breast tissue is lower than that of normal breast tissue, but the relative contents of NADH and flavin are larger in the cancerous breast tissue in comparison with the normal breast tissue. This observation is in good agreement with the pathological research results for cancerous and normal cells and tissues [3,5–7].

The most common breast cancer grading system currently used in the United States is the Scarff–Bloom–Richardson (SBR) system [3]. The SBR [3] or the modified SBR system [6,7] examines the cells and tissue structure of the breast cancer to determine how aggressive and invasive the cancer is depending on three features: (1) The percentage of the tumor in the tissue structures: in cancer, the tissue structures usually become less orderly. (2) The numbers of mitotic figures (dividing cells) observed in a certain magnitude microscope field: one of the hallmarks of cancer is that cells divide uncontrollably. (3) The nonuniformity of the cell nuclei: the cancerous cells have larger, more irregular, and darker cell nuclei than normal breast duct epithelial cells [3,6,7]. Each of these features is assigned a score ranging from 1 to 3. The lowest score 3 $(1 + 1 + 1)$ is given to well-differentiated tumors with the best prognosis while the highest score 9 $(3 + 3 + 3)$ is given for poorly differentiated tumors with the worst prognosis [3]. Breast tissue is mainly composed of an extracellular matrix of collagen fiber, fat, and epithelial cells. Epithelial cells, where cancer primarily happens, contain a number of endogenous fluorophores: tryptophan, NADH, flavin adenine dinucleotide (FAD), etc. [17]. NADH and FAD are involved in the oxidation of fuel molecules and can be used to probe changes in cellular metabolism [17]. Chance *et al.* exploited this phenomenon and showed that direct monitoring of NADH fluorescence dynamically interprets the metabolic activity within cells [18]. An intuitive application of the fluorescence spectroscopic technique is to study carcinogenesis in a variety of organ sites that are known to have increased metabolic rates, such as the breast [19]. All these features correspond to the description of SBR system: higher cell density, uncontrollable cell-dividing, and nonuniform larger cellular nuclei in cancerous breast cells. The primary fluorophore in the breast tissue extracellular matrix is type I collagen [20]. Fenhalls *et al.* investigated the relationship between synthesis of type I collagen and breast cancer stage [21]. For invasion and subsequent metastasis, tumor cells must degrade the surrounding extracellular matrix, which is composed mainly of type I collagen [21]. With grade advances, the cancer cells proliferate, increasing the cell density with nonuniform swelling

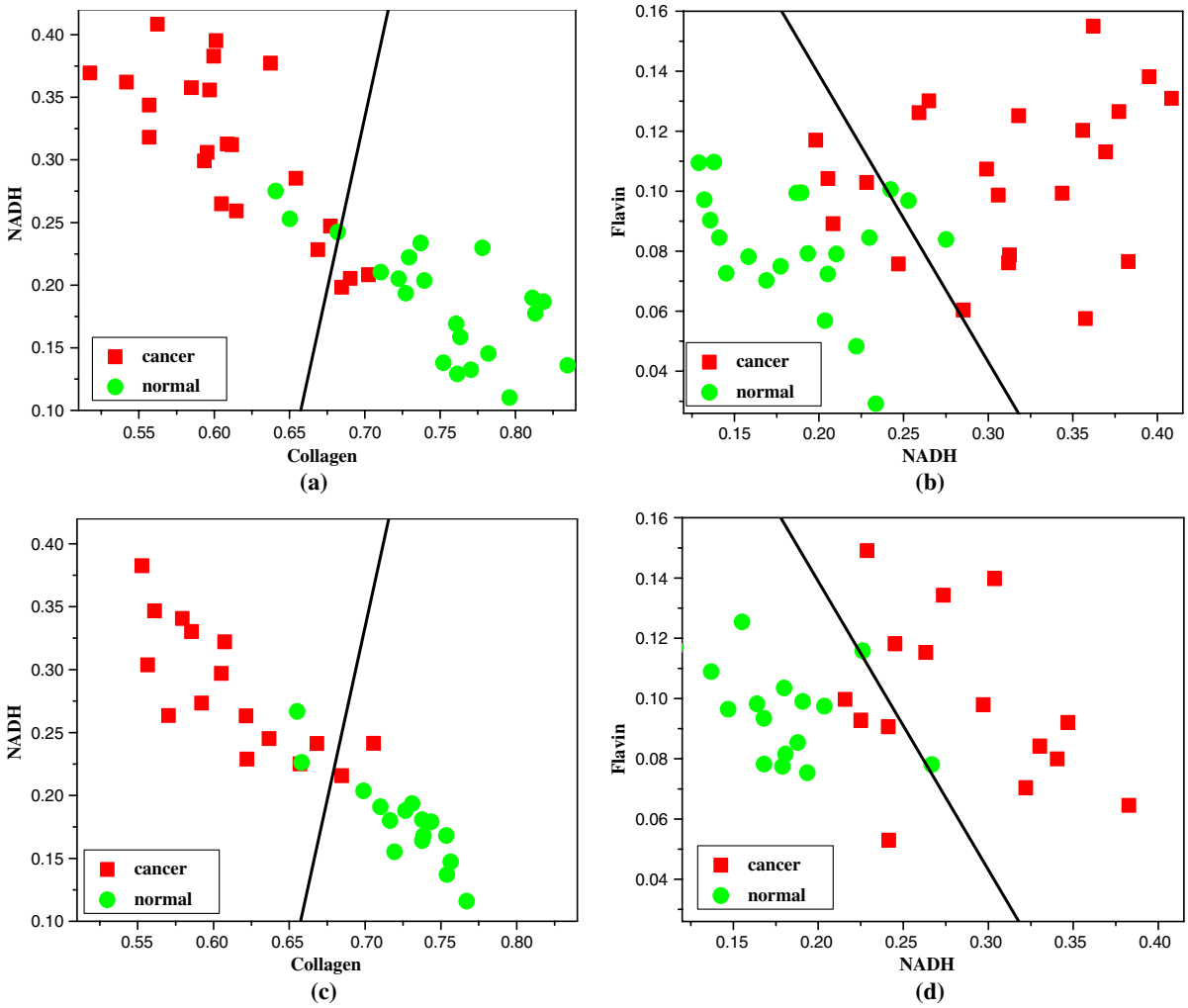

Fig. 3. (Color online) (a) Relative content of the first PC, collagen, versus that of the second PC, NADH. (b) Relative content of the second PC, NADH, versus that of the third PC, flavin, generated by analyzing emission spectra of the 22 pairs of cancerous and normal breast tissues obtained with the 340 nm excitation using the MCR-ALS method. The separating lines were calculated using the LDA method by treating the 22 pairs of data as training samples. The relative content extracted from 16 other pairs of data as testing samples for (c) collagen versus NADH, and (d) NADH versus flavin. They are used to evaluate performance and accuracy of the criteria separating lines generated by the LDA algorithm using the 22 training samples.

cellular nuclei and loss of collagen [21]. These changes during cancer evolution are critical to reveal the contributions of the biochemical components in tissue to their fluorescence spectra.

In a diagnosis test for cancer, the test outcome may be positive (cancer) or negative (healthy). To evaluate the potential of a diagnosis method, the following statistic terms are usually used: (1) true positive, defined as a cancerous sample correctly diagnosed as malignant; (2) false positive, defined as a healthy sample incorrectly identified as malignant; (3) true negative, defined as a healthy sample correctly identified as healthy; and (4) false negative, defined as a cancerous sample incorrectly identified as healthy. LDA is a method for finding a linear combination of features that separates two or more classes of objects or events [22]. The LDA method is usually useful for a two-group (class) case. The criteria for categorizing the true or false positive and negative groups in our study were first determined using the LDA algorithm and the 22 pairs of training data. The separating lines for the scatter plots, as shown in Figs. 3(a) and 3(b), were calculated using the LDA model for the diagnostically significant two pairs of fluorophores (PCs): collagen versus NADH and NADH versus flavin, respectively. The accuracy of the criteria and the potential of native fluorescence spectra and the MCR-ALS analysis combined with the LDA for effective diagnostic algorithms for breast tissue classification were then tested using 16 other pairs of data loaded into the subspace of corresponding pairs fluorophores, with the LDA separating line as the diagnostic criterion. The results are shown in Figs. 3(c) and 3(d). The sensitivity and specificity for distinguishing these 16 pairs of testing breast tissues using separating line generated with 22 pairs of training data were calculated and are summarized in Table 2.

Table 2. Sensitivity and Specificity of Classing Cancerous and Normal Breast Tissues Using Native Fluorescence Spectroscopy and the LDA Algorithm

Evaluated Components	Sensitivity (%)	Specificity (%)
Collagen versus NADH	85	85
NADH versus flavin	75	84

With the increasing of sample numbers, the diagnostic criterion generated by the LDA algorithm needs to be updated or modified. Theoretically, more data should result in a more accurate diagnostic criterion. On the other hand, more data to be trained may result in increasing the sensitivity and specificity until these values should keep unchanging or fluctuating very little. This indicates the limit of the native fluorescence spectroscopy and the MCR-ALS analysis combined with the LDA model for effective diagnostics of breast tissue. This classifier of the linear separating line obtained by LDA model can be expressed by $y = ax + b$. The LDA model was used for all available 38 data pairs to generate a separating line to improve diagnostic significance for using 22 pairs of fluorophores. The relative contents of collagen versus NADH, and NADH versus flavin for these 38 data pairs are shown as the scatter plots in Figs. 4(a) and 4(b), respectively. To compare the diagnostic criteria generated by different numbers of data, the separating lines obtained by the LDA using the 22 training data and all 38 data were loaded as solid and dashed lines, respectively, in Figs. 4(a) and 4(b).

It can be seen from Figs. 4(a) and 4(b) that the separating line generated by the LDA from both groups of data was very similar to its corresponding counterpart. The solid and dashed lines are close to overlapping. To compare the performance of the native fluorescence spectra and the LDA resulting

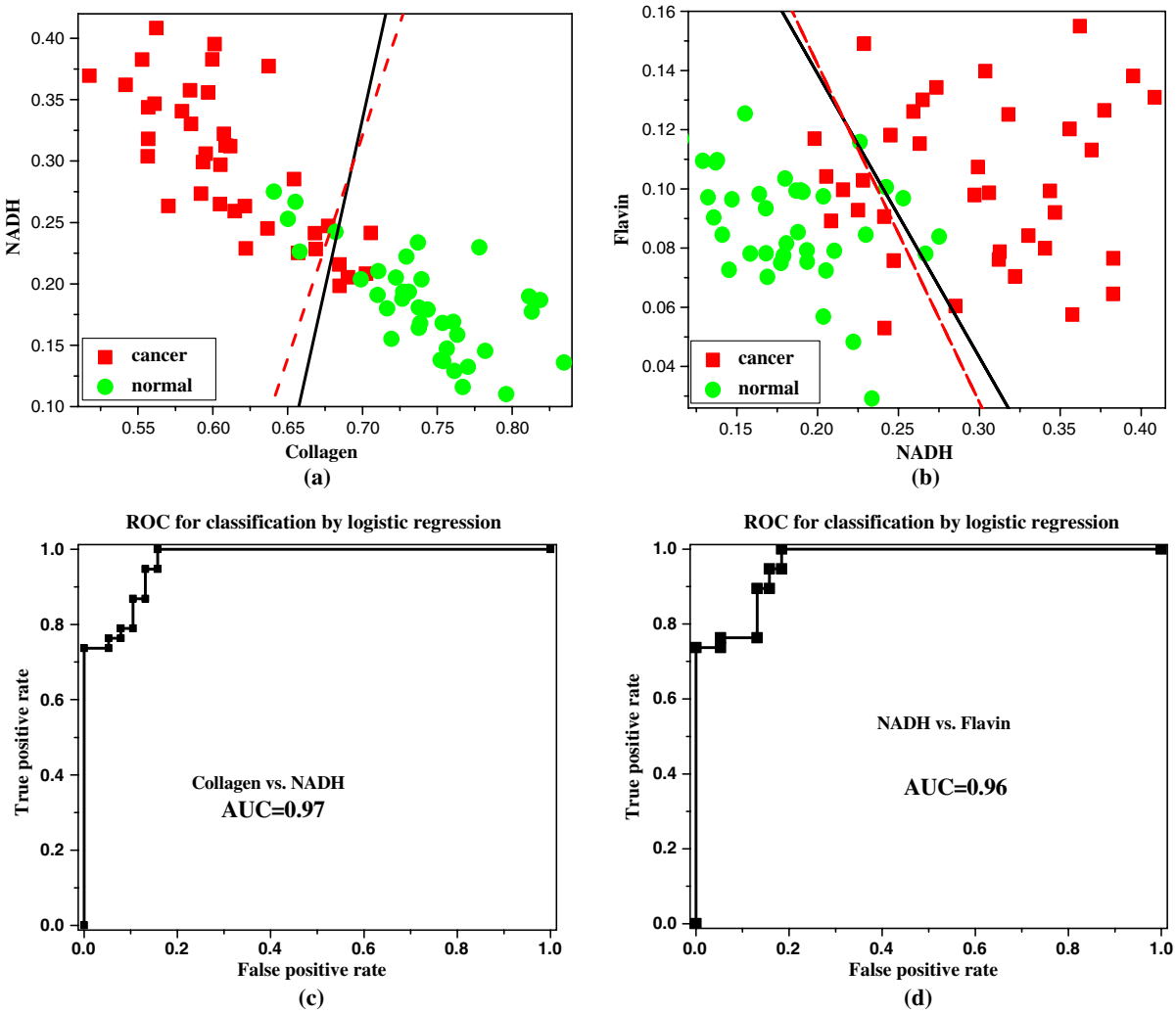

Fig. 4. (Color online) (a) Relative content of the first PC, collagen, versus that of the second PC, NADH. (b) Relative content of the second PC, NADH, versus that of the third PC, flavin, generated by analyzing emission spectra of the total 38 pairs of cancerous and normal breast tissues obtained with the 340 nm excitation using the MCR-ALS method. The separating lines were calculated using the LDA method. (c) ROC curve obtained using scatter plot of the first PC, collagen, versus the second PC, NADH. (d) ROC curve obtained using scatter plot of the second PC, NADH, versus the third PC, flavin, as the pairs of diagnostically significant fluorophores to evaluate performance of classifying breast tissues into two groups: cancer and normal.

from different groups of data, the criteria separating lines for these two groups of 22 and 38 data pairs are summarized in Table 3.

The performance of a two-group classification problem is typically evaluated with a ROC curve, which is a graphical plot of true positive rate versus false positive rate. The accuracy of the performance is measured by the area under the ROC curve (AUC). The ROC curves shown in Figs. 4(c) and 4(d) were generated from the scatter plots shown in Figs. 4(a) and 4(b), respectively, to determine the accuracy of classification for cancerous and normal breast tissues using different pairs of PCs. Figure 4(c) shows the ROC curve generated using the pairs of the first component (collagen) versus the second component (NADH), and 4(d) shows the ROC curve generated using the pairs of the second component (NADH) versus the third component (flavin). The AUC values of the ROC curves shown in Figs. 4(c) and 4(d) were calculated and listed in Table 3. In order to study the effect of the number of data to the value of AUC, the ROC curves were also generated from the scatter plot shown in Figs. 3(a) and 3(b) for the 22 data pairs, and the corresponding AUC values were calculated and listed in Table 3 for comparison with the results obtained from 38 pairs of data. The great AUC values demonstrate the excellent efficacy of using native fluorescence spectra and the MCR-ALS analysis combined with the LDA as a promising diagnostic tool for breast cancer detection [16].

The histological microscopy imaging measurements were performed to confirm our spectral study for breast cancer tissue. A number of stained histological slides corresponding to the pairs of the cancerous and normal tissues used for the spectral measurements were made by CHTN with a thickness of 250 μm for microscopy study. As an example, the microscopy images of an 85-year-old female with newly diagnosed breast cancer: ductal carcinoma *in situ* (DCIS) grade 3 were taken using a digital Binocular compound microscope (OMAX MD827S30) and compared with the results obtained from our spectral study. Figures 5(a) and 5(b) show the microscopy images (using 40× objective) of the cancerous and normal breast tissues, respectively. Figures 5(c) and 5(d) exhibit fluorescence spectra of the cancerous and normal breast tissues from the same patient. Comparing Figs. 5(c) and 5(d) with Fig. 1, the reproducible results were observed. The major difference between the fluorescence spectral profiles of the cancerous and normal breast tissues is the existence of a much stronger shoulder peak at ~440 nm for the cancerous tissue in comparison with the normal tissue. This difference indicates the reduced relative content of collagen, which contributes to the peak at ~380 nm and the increased relative content of NADH, which contributes to the peak at ~440 nm to ~460 nm.

For readers in the biomedical optics field, the following pathology reports provided by CHTN for the breast cancer sample corresponding to the investigated slides may be of interest: (1) metastatic ductal carcinoma in eight of eight axillary lymph nodes with extensive extranodal extension (8/8), involving the deep margin of the axillary tail; (2) invasive ductal carcinoma, at least 4.0 cm, poorly differentiated, micropapillary type, numerous microscopic foci of skip satellite lesions near the main mass (central) as well as upper inner and lower inner quadrants; (3) DCIS grade 3, estrogen receptor positive (ER+), human epidermal growth factor receptor 2 positive (HER2+) at least tumor initiating cell; and (4) specimen margin, by total mastectomy, the antero-superior margin negative ≥0.2 cm from the invasive carcinoma or DCIS and the antero-inferior margin negative ≥0.2 cm from the invasive carcinoma or DCIS.

4. Discussion

It is well-known that no native fluorophores emit in the infrared spectral range. Most fluorophores emit in the UV to visible range. As indicated in Table 1, light at 340 nm can be used to effectively excite three native fluorophores (collagen, NADH, and flavin), which may be good candidate biomarkers for cancer detection [10–12]. There are three types of UV rays: UVA (400–320 nm), UVB (320–280 nm), and UVC (280–100 nm). Although exposure to too many UV rays can cause cancer, the Federation of American Societies for Experimental Biology indicated that the most damaging types of UV light are UVB and UVC, not UVA [15]. Unlike UVB and UVC, UVA does not damage DNA directly. The body finds it harder to repair damage, including harm to DNA, caused by UVB rays. The mutations to the fibroblasts caused by UVB were more prevalent. The UVA-induced oxidized purines can be repaired rapidly [15] so the mutagenicity can be controllable.

Based on extensive epidemiologic studies of skin cancer incidence, Urbach studied the biologically effective UV to be the cause of the skin cancer incidence [23]. The measurements of the action spectrum of mouse skin carcinogenesis and human skin erythema show that the spectral effectiveness is maximized at 300 nm, decreases rapidly with longer wavelength, and becomes negligible for the wavelengths longer

Table 3. Comparison of Criteria Separating Lines and AUC Using 22 and 38 data Pairs for Cancerous and Normal Breast Tissues

Evaluated Components	Group of Data	Separating Line	AUC
Collagen versus NADH	22 pairs of training data	$y = 5.5x - 3.5$	0.96
	38 pairs of evaluated data	$y = 3.6x - 2.2$	0.97
NADH versus flavin	22 pairs of training data	$y = -0.96x + 0.33$	0.95
	38 pairs of evaluated data	$y = -1.1x + 0.37$	0.96

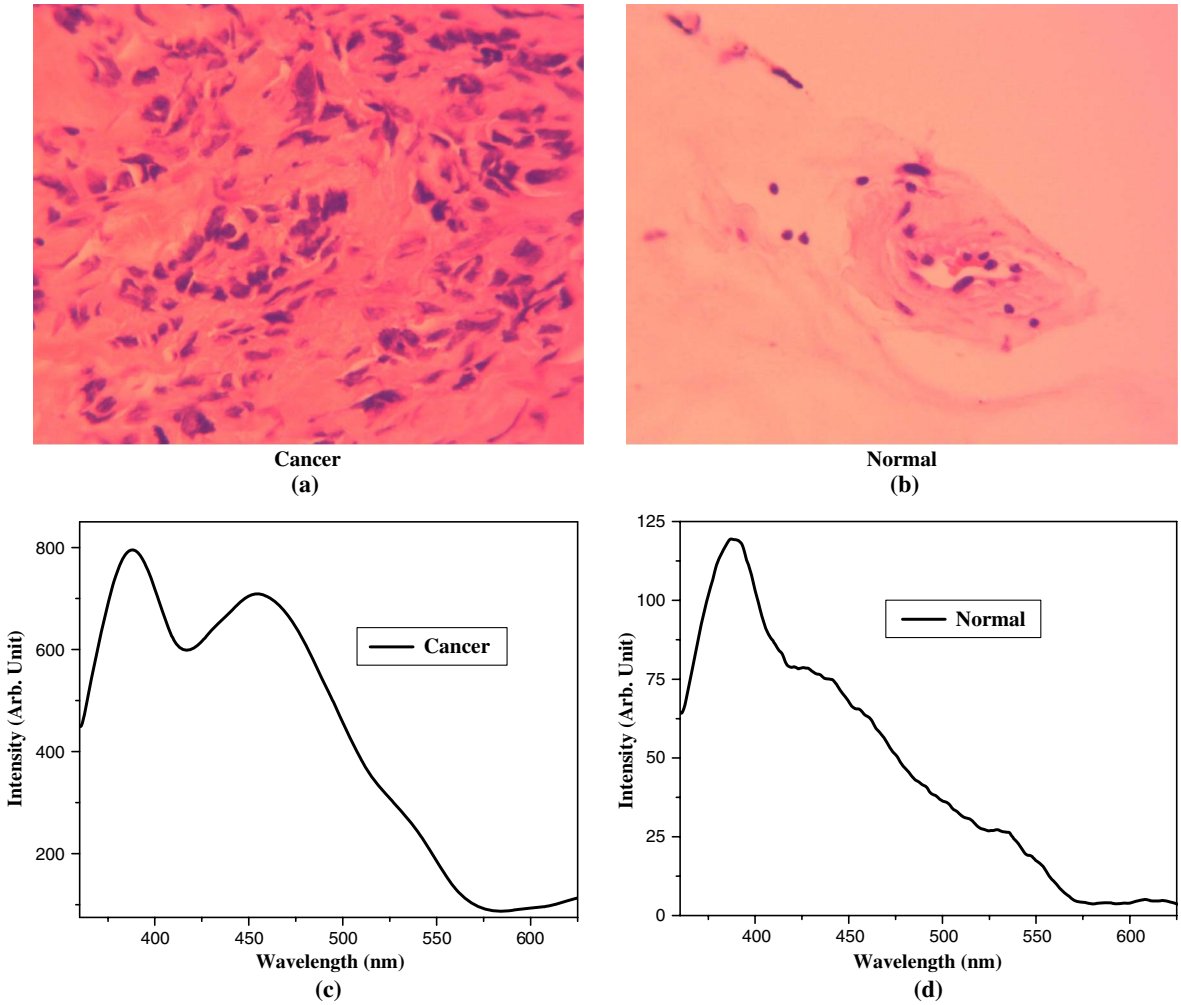

Fig. 5. (Color online) Microscopic images of the (a) cancerous and (b) normal breast tissue samples. The magnificent factor for microscopic images is 40×. The cancer is diagnosed as DCIS grade 3 by a pathology medical doctor. The fluorescence spectra of (a) cancerous and (b) normal breast tissues were obtained with the excitation of 340 nm.

than 360 nm [23]. Based on the data shown in Fig. 3 of Urbach's paper [23], which indicates spectral action for mouse skin carcinogenesis and human erythema, the spectral effectiveness for carcinogenesis at 340 nm is 1.58×10^{-3} times smaller than that at 300 nm. In addition, during fluorescence measurements with 340 nm excitation, the carcinogenesis risk for patients can be controlled by changing the excitation dosage levels and scanning time. As a result, the selected excitation wavelength of 340 nm may be safe and has the potential to be used in clinical study in future.

5. Conclusion

Changes of fluorescence spectra acquired with the selective excitation wavelength of 340 nm were observed for the cancerous breast tissue compared with the normal tissue. This research demonstrates that the native fluorescence spectroscopy may be used to investigate the changes of the relative contents of the key native fluorophores between cancerous and normal breast tissues. The results analyzed with the MCR-ALS method indicate that the changes of fluorescence spectra of the cancerous tissue compared with the normal tissue are caused by reduced contribution of collagen and increased contribution of NADH and flavin. Differentiation between cancerous and normal breast tissues can be achieved by using native fluorescence spectra and the MCR-ALS analysis combined with the LDA. Since it is important to yield minimal photo-toxicity and cause no mutagenicity in human model in clinic, the native fluorescence spectroscopy with the selected excitation wavelength of 340 nm may present a better diagnostic method to differentiate the diseased tissue from healthy tissue and may be applied for *in vivo* breast cancer detection. The native fluorescence spectroscopy may have potential to be developed into a new armamentarium.

This research is supported in part by U. S. Army Medical Research and Material Command (USAMRMC) under Grant Nos. W81XWH-11-1-0335 (CUNY RF No. 47204-00-01) and W81XWH-08-1-0717 (CUNY RF No. 47170-00-01). Yang Pu acknowledges the useful discussion with Laura A. Sordillo for

the selection of excitation wavelength of 340 nm over 300 nm. The authors acknowledge the help of CHTN and NDRI for providing normal and cancerous breast tissue samples for the measurements.

References

1. American Cancer Society, "Cancer facts & figures 2012," Atlanta: American Cancer Society (2012).
2. R. W. Scarff and H. Torloni, "Histological typing of breast tumors," in *International Histological Classification of Tumours* (World Health Organization, 1968).
3. H. J. G. Bloom and W. W. Richardson, "Histological grading and prognosis in breast cancer; a study of 1409 cases of which 359 have been followed for 15 years," Br. J. Cancer **11**, 359–377 (1957).
4. C. W. Elston, "The assessment of histological differentiation in breast cancer," Aust. N. Z. J. Surg. **54**, 11–15 (1984).
5. C. W. Elston and I. O. Ellis, "Pathological prognostic factors in breast cancer. I. The value of histological grade in breast cancer: experience from a large study with long-term follow-up," Histopathology **19**, 403–410 (1991).
6. I. Balslev, C. K. Axelsson, K. Zedeler, B. B. Rasmussen, B. Carstensen, and H. T. Mouridsen, "The Nottingham Prognostic Index applied to 9,149 patients from the studies of the Danish Breast Cancer Cooperative Group (DBCG)," Breast Cancer Res. Treat. **32**, 281–290 (1994).
7. J. F. Simpson, R. Gray, L. G. Dressler, C. D. Cobau, C. I. Falkson, K. W. Gilchrist, K. J. Pandya, D. L. Page, and N. J. Robert, "Prognostic value of histologic grade and proliferative activity in axillary node-positive breast cancer: results from the eastern cooperative oncology group companion study, EST 4189," J. Clin. Oncol. **18**, 2059–2069 (2000).
8. R. R. Alfano, D. Tata, J. Cordero, P. Tomashefsky, F. Longo, and M. Alfano, "Laser induced fluorescence spectroscopy from native cancerous and normal tissue," IEEE J. Quantum Electron. **20**, 1507–1511 (1984).
9. R. R. Alfano, G. C. Tang, A. Pradhan, W. Lam, D. S. J. Choy, and E. Opher, "Fluorescence spectra from cancerous and normal human breast and lung tissues," IEEE J. Quantum Electron. **QE-23**, 1806 –1811 (1987).
10. Y. Pu, W. B. Wang, Y. Yang, and R. R. Alfano, "Stokes shift spectroscopy highlights differences of cancerous and normal human tissues," Opt. Lett. **37**, 3360–3362 (2012).
11. A. S. Haka, K. E. Shafer-Peltier, M. Fitzmaurice, J. Crowe, R. R. Dasari, and M. S. Feld, "Diagnosing breast cancer by using Raman spectroscopy," Proc. Natl. Acad. Sci. USA **102**, 12371–12376 (2005).
12. Y. Pu, W. Wang, G. Tang, and R. R. Alfano, "Changes of collagen and nicotinamide adenine dinucleotide in human cancerous and normal breast tissues studied using fluorescence spectroscopy with selective excitation wavelength," J. Biomed. Opt. **15**, 047008 (2010).
13. Y. Pu, W. B. Wang, B. B. Das, and R. R. Alfano, "Time-resolved spectral wing emission kinetics and optical imaging of human cancerous and normal prostate tissues," Opt. Commun. **282**, 4308–4314 (2009).
14. R. Tauler, M. Maeder, and A. de Juan, "Multi-set data analysis: extended multivariate curve resolution," *Comprehensive Chemometrics* (Elsevier, 2009), pp. 473–506.
15. A. Besaratinia, S. Kim, and G. P. Pfeifer, "Rapid repair of UVA-induced oxidized purines and persistence of UVB-induced dipyrimidine lesions determine the mutagenicity of sunlight in mouse cells," FASEB J. **22**, 2379–2392 (2008).
16. Y. Sun, Y. Pu, Y. Yang, and R. R. Alfano, "Biomarkers spectral subspace for cancer detection," J. Biomed. Opt. **17**, 107005 (2012).
17. D. L. Heintzelman, R. Lotan, and R. R. Richards-Kortum, "Characterization of the autofluorescence of polymorphonuclear leukocytes, mononuclear leukocytes and cervical epithelial cancer cells for improved spectroscopic discrimination of inflammation from dysplasia," Photochem. Photobiol. **71**, 327–332 (2000).
18. B. Chance, J. R. Williamson, D. Famieson, and B. Schoener, "Properties and kinetics of reduced pyridine nucleotide fluorescence of the isolated and in vivo rat heart," Biochem. Z. **341**, 357–377 (1965).
19. D. K. Bird, L. Yan, K. M. Vrotsos, K. W. Eliceiri, E. M. Vaughan, P. J. Keely, J. G. White, and N. Ramanujam, "Metabolic mapping of MCF10A human breast cells via multiphoton fluorescence lifetime imaging of the coenzyme NADH," Cancer Res. **65**, 8766–8773 (2005).
20. Y. Pu, G. C. Tang, W. B. Wang, H. E. Savage, S. P. Schantz, and R. R. Alfano, "Native fluorescence spectroscopic evaluation of chemotherapeutic effects on malignant cells using nonnegative matrix factorization analysis," Technol. Cancer Res. Treat. **10**, 113–120 (2011).
21. G. Fenhalls, D. M. Dent, and M. I. Parker, "Breast tumour cell-induced down-regulation of type I collagen mRNA in fibroblasts," Br. J. Cancer **81**, 1142–1149 (1999).
22. Y. Pu, W. B. Wang, Y. Yang, and R. R. Alfano, "Stokes shift spectroscopic analysis of multi-fluorophores for human cancer detection in breast and prostate tissues," J. Biomed. Opt. **18**, 017005 (2013).
23. F. Urbach, "Potential effects of altered solar ultraviolet radiation on human skin cancer," Photochem. Photobiol. **50**, 507–513 (1989).